Optimization of Methyl-Ammonium Tin Iodide Perovskite Solar Cells with Molybdenum Trioxide as a Front Contact

*Faruk Sani
Department of Physics, Usmanu Danfodiyo University,
2346, Sokoto, Nigeria.
*Corresponding author: faruk.sani@udusok.edu.ng

Abstract
Indium-doped tin oxide (ITO) is the most common transparent conductive oxide layer used as front contact in perovskite-based solar cells. However, due to the high cost of indium, it is imperative to further explore alternative front contact in perovskite solar cells. In this study, lead-free perovskite solar cell in planar configuration; $MoO_3/TiO_2/CH_3NH_3SnI_3$/Spiro-OMeTAD/Au was designed and studied using SCAPS software. In order to achieve an optimum performance, MoO_3 and $CH_3NH_3SnI_3$ layer thickness were varied and studied. The simulation results show no significance effect on the efficiency of the devices when the MoO_3 thickness increased from 100 nm to 1000 nm. Moreover, the results also show that the efficiency of the devices is exclusively depends on the absorber layer thickness. The $CH_3NH_3SnI_3$ layer exhibited the optimum performance at 700 nm with short circuit current (J_{SC}), open circuit voltage (V_{OC}), fill factor (FF) and power conversion efficiency (PCE) of 33.5566 mA/cm^2, 0.9722 V, 80.38 %, and 26.22 % respectively. The results obtained show the possibility of designing and fabricating tin-based perovskite solar cells with MoO_3 as a front contact.
Keywords: efficiency; molybdenum trioxide; perovskite; thickness; tin.

Introduction

Perovskite based solar cells have revealed momentous development of power conversion efficiency (PCE) in less than two decades from initial efficiency of 3.8 % [1] to 25.6 % [2]. This outstanding performance is attained owing to their unique properties such as direct and tunable band, high absorption co-efficient, excellent charge carrier mobility, long diffusion length, and simple methods of production [3 - 4]. However, one of the major issues of concern is the used of toxic divalent lead (Pb^{2+}) cation in the perovskite absorber layer. Hence, it is imperative to explore an alternative non divalent metal to lead (Pb^{2+}). One of the suitable divalent metals to replace Pb^{2+} is tin (Sn^{2+}) due to their comparable electronic configuration and close effective ionic radius [5 - 6].

Perovskite solar cell (PSC) is made up of various layers on top of a substrate. Transparent conductive oxide layer (TCO) is one of the basic layers in PSCs and has significant impact on the efficiency and stability of the device. TCO can only achieve best performance, if it possesses a band gap energy of greater than or equal to 3.1 eV [7]. The most common commercial TCO used in PSC is indium-doped tin oxide (ITO) due to its excellent properties such as high transmittance and low resistivity [8, 9]. However, indium can easily migrate from ITO into the perovskite absorber layer, results instability in PSCs [10]. Moreover, indium metal is non abundant, costly and toxic [11 -12].In this numerical study, we examined the possibility of using MoO_3 as a front contact for tin-based perovskite solar cells with a configuration; MoO_3(TCO)/TiO_2/$CH_3NH_3SnI_3$/Spiro-OMeTAD/Au by varying the thickness of the MoO_3 and $CH_3NH_3SnI_3$ layer using SCAPS.

Materials and Methods
Materials
The perovskite –based solar structure adopted in this simulation is MoO$_3$ /TiO$_2$/CH$_3$NH$_3$SnI$_3$/Spiro-OMeTAD/Au. The materials used for this simulation are MoO$_3$ and Au as a front contact and back contact respectively, TiO$_2$ and Spiro-OMeTAD used as a electron transporting layer and hole transporting layer respectively, and CH$_3$NH$_3$SnI$_3$ acted as the light absorbing material. The input parameters used for these layers are tabularized in Table 1.

Table 1: Input parameters used for the simulation

Input Parameters	MoO$_3$	TiO$_2$	CH$_3$NH$_3$SnI$_3$	Spiro-OMeTAD
Thickness (nm)	100 varied	100	500 varied	200
Band gap (eV)	3.8	3.2	1.3	3.0
Electron affinity (eV)	4.1	3.9	4.17	2.45
Dielectric permittivity	9.0	9.0	8.2	3.0
CB effective density of state (cm^{-3})	2.2 x 10^{18}	1 x 10^{21}	1 x 10^{18}	1 x 10^{19}
VB effective density of state (cm^{-3})	1 x 10^{19}	2 x 10^{20}	1 x 10^{18}	1 x 10^{19}
Electron mobility (cm^{2}s^{-1})	30	20	1.6	0.0002
Hole mobility (cm^{2}s^{-1})	6	10	1.6	0.0002
Donor density (cm^{-3})	1 x 10^{17}	1 x 10^{19}	0	0
Acceptor density (cm^{-3})	0	0	1 x 10^{16}	1 x 10^{18}
Defect density (cm^{-3})	1 x 10^{14}	1 x 10^{15}	1 x 10^{15}	1 x 10^{15}

Methods
In this work, the simulation and the analysis were carried out using Solar Capacitance Simulation (SCAPS) software. AM1.5G solar illumination with an incident power density of 1000 W/cm^2 (1 Sun) was adopted from the software and the physical parameters listed in Table 1.1. SCAPS-1D is designed and developed at the University of Gent, Belgium. It works by solving the three basic equations for semiconductors; Poisson equations, the continuity equations for electrons, and holes and carrier transport [13]. The SCAPS interface is presented in Figure 1.
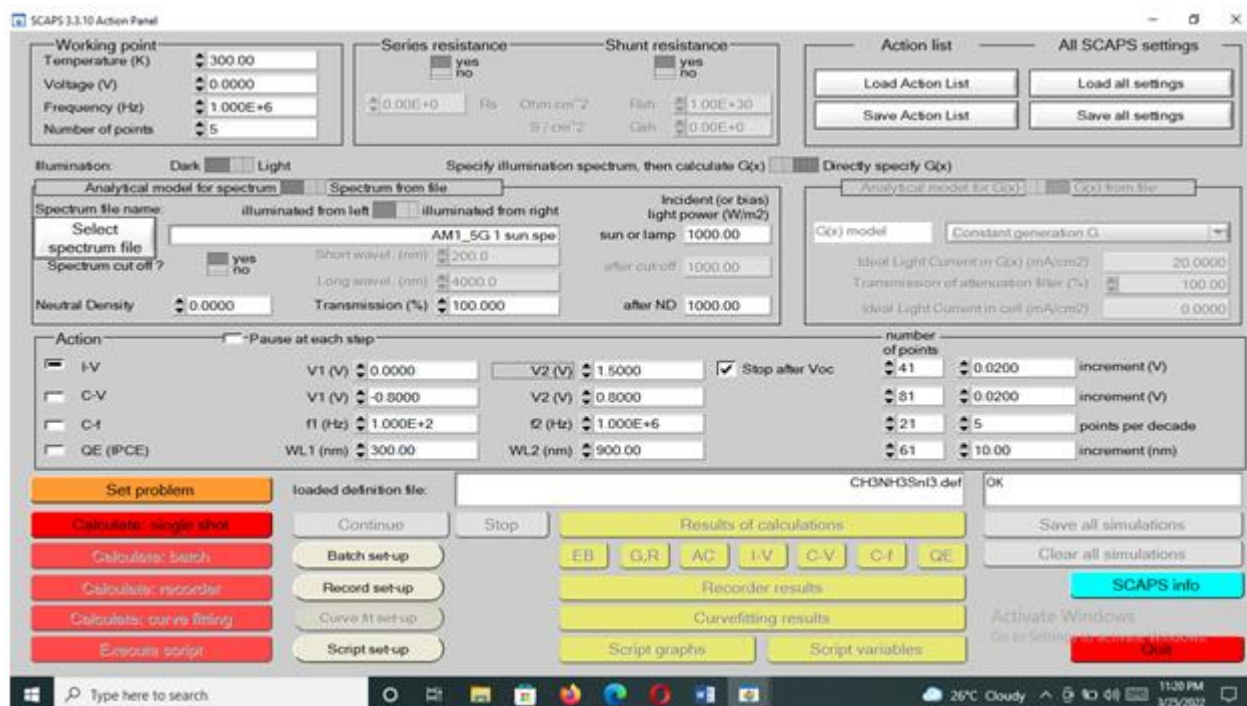

Figure 1 The SCAPS interface.

Results and discussion
Effect of the absorber layer thickness
In order to investigate the effect of the absorber layer thickness on the performance of the devices, the thickness of the $CH_3NH_3SnI_3$ was varied from 100 nm to 1000 nm while the remaining input parameters tabulated in Table 1 kept constant. Table 2 presents the photovoltaic parameters obtained for the devices. From Table 2 (a), it could be observed that V_{OC} slowly decreases with the increase in the absorber layer thickness. This drop of the V_{OC} might be due to the increase in band gap of the absorber layer as the thickness increases as reported by [14]. The J_{SC} increases rapidly from 16.6863 mA/cm^2 to 33.82mA/cm^2 as the thickness increased from 100 nm to 1000 nm. This rapid increase in J_{SC} is due to the increase in the generation of carrier concentration by the absorber layer. The PCE rises from 13.86 % and peaks at 26.22 % and then gradually decreased. From the results obtained, the desirable thickness of the $CH_3NH_3SnI_3$ layer is 700 nm.

Effect of the TCO layer thickness
The effect of MoO_3 layer thickness was studied and discussed. The MoO_3 thickness was varied from 100 nm to 1000 nm and the rest of the input parameters kept constant. Table 2 (b) presented the electrical outputs obtained. It could be seen from the Table 2 (b) that no significant change in PCE is observed as the thickness of the MoO_3 increased from 100 nm to 1000 nm. This indicates that MoO_3 thickness could not influence the device performance. This simulation shows the possibility of using MoO_3 as a front contact to achieve inexpensive and stable tin-based perovskite solar cells.

Table 2: Electrical output obtained at (a) $CH_3NH_3SnI_3$ thicknesses and (b) MoO_3 thicknesses

(a) CH₃NH₃SnI₃ thicknesses

Thickness (nm)	Voc (V)	Jsc (mA/cm^2)	FF (%)	PCE (%)
100	1.0091	16.6863	82.32	13.86
200	0.9965	24.6866	82.28	20.28
300	0.9888	28.8561	82.32	23.49
400	0.9830	31.1543	81.99	25.11
500	0.9785	32.4525	81.38	25.84
600	0.9750	33.1747	80.84	26.15
700	0.9722	35.5566	80.38	26.22
800	0.9701	33.7403	80.01	26.18
900	0.9684	33.8117	79.74	26.10
1000	0.9671	33.8228	79.53	26.02

(b) MoO₃ thicknesses

Thickness (nm)	Voc (V)	Jsc (mA/cm^2)	FF (%)	PCE (%)
100	0.9785	32.4525	81.38	25.84
200	0.9785	32.4484	81.38	25.84
300	0.9785	32.4448	81.38	25.84
400	0.9785	32.4411	81.38	25.83
500	0.9785	32.4380	81.38	25.83
600	0.9785	32.4351	81.38	25.83
700	0.9785	32.4324	81.38	25.83
800	0.9785	32.4299	81.38	25.82
900	0.9785	32.4277	81.38	25.82
1000	0.9785	32.4256	81.38	25.82

Conclusion

In this work, lead-free perovskite solar cell in planar configuration; $MoO_3/TiO_2/CH_3NH_3SnI_3/Spiro$-OMeTAD/Au was designed and studied using SCAPS software. MoO_3 and $CH_3NH_3SnI_3$ thicknesses were varied from 100 nm to 1000 nm to investigate their influence on the efficiency of the devices. From our simulation results, no significance effect on the efficiency of the devices was observed as the MoO_3 thickness increased from 100 nm to 1000 nm. However, the results also reveal that the efficiency of the device is solely depends on the absorber layer thickness. The $CH_3NH_3SnI_3$ layer exhibited the optimum performance at 700 nm with J_{SC}, V_{OC}, FF and PCE of 33.5566 mA/cm^2, 0.9722 V, 80.38 %, and 26.22 % respectively. The results obtained show the possibility of designing and fabricating low cost and stable tin-based perovskite solar cells with MoO_3 as a front contact.

Acknowledgement

References

[1] Kojima. A.; Teshima. K.; Shirai, Y.; and Miyasaka T. 2009. Organometal Halide Perovskites as Visible-Light Sensitizers for Photovoltaic Cells. *Journal of American Chemical Society*, *131*, 6050–6051.

[2] Pv magazine. https://www.pv-magazine.com/2021/04/06/unist-epfl-claim-25-6-efficiency-world-record for-perovskite-solar-cell/ (Retrieved February 15, 2022).

[3] Chen. Q.; Marco. N.D.; Yang. Y.; Song. T.B.; Chen. C.C.; Zhou. H.; Yang. Y. 2015. Under the Spotlight: The Organic-Inorganic Hybrid Halide Perovskite for Optoelectronic Applications. *Nano Today*,10, 355-396.

[4] Green. M. A.; Ho-Baillie, A.; and Snaith. H. J. 2014. The emergence of perovskite solar cells. *Nature Photonics*, *8*(7), 506–514.

[5] Nagabhushana. G. P.; Shivaramaiah. R.; and Navrotsky. A. 2016. Direct calorimetric verification of thermodynamic instability of lead halide hybrid perovskites. *Proceedings of the National Academy of Sciences*, 113(28), 7717–7721.

[6] Hoefler. S. F.; Trimmel. G.; and Rath. T. 2017. Progress on Lead-free Metal Halide Perovskites for Photovoltaic Applications: A Review. *Monatshefte Fur Chemie*, 148(5), 795–826.

[7] Guillén, C. and Herrero, J. 2011. TCO/metal/TCO structures for energy and flexible electronics. *Thin Solid Films*, 520, 1–17. http://dx.doi.org/10.1016/j.tsf.2011.06.091.

[8] Noel, N.K.; Stranks, S.D.; Abate, A.; Wehrenfennig, C.; Guarnera, S.; Haghighirad, A.-A.; Sadhanala, A.; Eperon, G.E.; Pathak, S.K.; Johnston, M.B. 2014. Lead-free organic– inorganic tin halide perovskites for photovoltaic applications. *Energy Environ. Sci.*, 7, 3061–3068.

[9] Hao, F.; Stoumpos, C.C.; Cao, D.H.; Chang, R.P.; Kanatzidis, M.G. 2014. Lead-free solid-state organic–inorganic halide perovskite solar cells. *Nat. Photonics*, 8, 489.

[10] Way. A., Luke, J., Evans, A.D., Li, Z., Kim, J-S., Durrant, J.R., Lee, H.K.H. and Tsoi, W.C. 2019. Fluorine doped tin oxide as an alternative of indium tin oxide for bottom electrode of semi-transparent organic photovoltaic devices, *AIP Advances,* 9 (8), http://doi.org/10.1063/1.5104333.

[11] Dianetti, M., Di Giacomo, F., Polino, G., Ciceroni, C., Liscio, A., D'Epifanio, A., Licoccia, S., Brown, T.M., Di Carlo, A., Brunetti, F. 2015. TCO-free flexible organo metal trihalide perovskite planar-heterojunction solar cells. Sol. *Energy Mater. Sol. Cells,* 140, 150–157.

[12] Hagendorfer, H., Lienau, K., Nishiwaki, S., Fella, C.M., Kranz, L., Uhl, A.R., Jaeger, D., Luo, L., Gretener, C., Buecheler, S., Romanyuk, Y.E., Tiwari, A.N. 2014. Highly transparent and conductive ZnO: Al thin films from a low temperature aqueous solution approach. *Adv. Mater.*, 26, 632–636.

[13] Movla, H. 2014. Optimization of the CIGS based thin film solar cells: numerical simulation and analysis. *Optik*, vol. 125, no. 1, pp. 67–70.

[14] Bag. A.; Radhakrishnan. R.; Nekovei. R. and Jeyakumar, R. 2020. Effect of absorber layer, hole transport layer thicknesses, and its doping density on the performance of perovskite solar cells by device simulation. *Solar Energy,* vol. 196, pp. 177–182.